UHASSELT
KNOWLEDGE IN ACTION

Maastricht University

Faculty of Medicine and Life Sciences
School for Life Sciences
Master of Biomedical Sciences

Master's thesis

Validation of preclinical cellular models to screen the effectiveness of drugs directed to slow down Alzheimers and Parkinsons disease progression

Anaïs Luykx

Thesis presented in fulfillment of the requirements for the degree of Master of Biomedical Sciences, specialization Molecular Mechanisms in Health and Disease

SUPERVISOR :
Prof. dr. Ilse DEWACHTER

SUPERVISOR :
dr. Jolien BEEKEN

MENTOR :
Teun VAN NUNEN

2022
2023

UHASSELT
KNOWLEDGE IN ACTION

www.uhasselt.be
Universiteit Hasselt
Campus Hasselt:
Martelarenlaan 42 | 3500 Hasselt
Campus Diepenbeek:
Agoralaan Gebouw D | 3590 Diepenbeek

UHASSELT
KNOWLEDGE IN ACTION

Maastricht University

Faculty of Medicine and Life Sciences
School for Life Sciences
Master of Biomedical Sciences

Master's thesis

Validation of preclinical cellular models to screen the effectiveness of drugs directed to slow down Alzheimers and Parkinsons disease progression

Anaïs Luykx

Thesis presented in fulfillment of the requirements for the degree of Master of Biomedical Sciences, specialization Molecular Mechanisms in Health and Disease

SUPERVISOR :
Prof. dr. Ilse DEWACHTER

SUPERVISOR :
dr. Jolien BEEKEN

MENTOR :
Teun VAN NUNEN

Validation of preclinical cellular models to screen the effectiveness of drugs directed to slow down Alzheimer's and Parkinson's disease progression

Anaïs Luykx[1], Teun van Nunen[1], and Jolien Beeken[1,2]

[1]Neurology research group, Innoser, Agoralaan A bis, 3590 Diepenbeek
[2]Cardiometabolic diseases research group, Innoser, Agoralaan A bis, 3590 Diepenbeek

Running title:** ***A preclinical model to screen drug's effectiveness

To whom correspondence should be addressed: Jolien Beeken, Tel: +32 470 86 13 31; Email:jbeeken@innoserlaboratories.com

Keywords: SH-SY5Y cells, HMC3 cells, Phagocytosis, Cell viability, Alzheimer's Disease, Parkinson's Disease

ABSTRACT

Alzheimer's (AD) and Parkinson's (PD) disease drug development is held back due to the lack of *in vitro* reproducible models that represent human complexity. These models can be used to screen disease-modifying therapeutics relatively inexpensively, efficiently, and fast. Most therapies for neurodegenerative diseases (NDD) currently focus on relieving symptoms rather than preventing disease progression. New and more powerful therapeutic approaches targeting disease pathology are needed to address the acceleration and severity of NDD. Our research goal is to validate *in vitro* disease-induced cell models of neuronal and microglial cell cultures and eventually co-cultures to screen disease-modifying drugs for NDDs prior to screening *in vivo*. Cell viability and phagocytosis are two significant players in the progression of NDD caused by fibril aggregation and are used as main readouts for our disease models. Microglial (HMC3) and differentiated neuronal-like cells (SH-SY5Y) were treated with pre-formed fibrillar Amyloid beta (fAβ) or alpha-Synuclein (fαSyn) to mimic AD and PD pathophysiology, respectively. Results showed that our models represented phagocytosis of fibrils which was increased upon aducanumab treatment in our fAβ AD model. Furthermore, after fAβ and fαSyn treatment our cellular model showed a decrease in cell viability as seen with NDD. Our NDD models of pre-formed fibril treatment on HMC3 and SH-SY5Y cells will serve as a cheaper, easier, and faster alternative model to screen AD and PD disease-modifying drugs before screening *in vivo*.

INTRODUCTION

Neurodegenerative diseases (NDDs) are predicted to become the top 2 causes of death in elderly in 20 to 30 years due to population aging. NDDs are hallmarked as a condition in which central nervous system (CNS) cells cease functioning or even die. NDDs are incurable diseases that deteriorate with time, and the majority of treatments currently focus on alleviating the patient's symptoms rather than blocking the development of the disease (1, 2). Despite the variety of their etiology, numerous NDDs share comparable features, including the increased buildup of misfolded proteins, oxidative stress, and neuroinflammation, that all contribute to neuronal dysfunction and cell death (1, 3).

The most common NDD is **Alzheimer's disease (AD),** affecting around 55 million people worldwide (4). AD symptoms consist of memory loss, and cognitive difficulties such as wandering and getting lost, repetition in speaking and having difficulties with routine daily tasks that are greater than the cognitive changes expected with normal aging (1). AD is characterized by the formation of extracellular plaques of β-amyloid peptide (Aβ-plaques) and the presence of intracellular neurofibrillary tangles (NFT). The proteolytic

degradation of the amyloid precursor protein (APP) by β- and γ -secretases results in these Aβ fibrils that consist of 40-42 amino acid peptides, while NFTs are composed of hyperphosphorylated and misfolded protein tau (5, 6). Here, we focus on the Aβ plaques which accumulate in the brain of AD patients. The physiological role of Aβ is not known, and depending on the γ-secretase location, different Aβ peptides can be produced, such as Aβ40 and Aβ42 (7). In humans, the Aβ40 peptide, which is 40 amino acids (AA) long, is more common than the Aβ42 peptide, a 42 AA long fragment with 2 additional AA residues at the C-terminus. Aβ42 is more prone to oligomerize and diffuse into synaptic clefts and interfere with synaptic signalling (6). However, both Aβ42 and Aβ40 polymerize into insoluble amyloid fibrils that aggregate into Aβ-plaques. The higher the ratio of Aβ42/Aβ40, the more severe the AD progression (5, 6). Furthermore, amyloid plaques are believed to cause degeneration of pyramidal neurons in the basal forebrain and hippocampus, by inducing neuronal injury and subsequently neuronal death which causes learning and memory problems (1) (**Figure 1**, left panel).

Parkinson's Disease (PD) is the second most prevalent NDD, affecting around 10 million individuals globally (8). Motor impairment, including bradykinesia, rest tremor, stiffness, and changes in posture and gait, as well as cognitive impairment, including memory loss, are the most occurring PD symptoms. One pathological hallmark of PD is the neuronal inclusion in the form of Lewy bodies and Lewy neurites. Lewy bodies are constituted out of misfolded intracellular alpha-synuclein (αSyn) species. The aggregation process of αSyn into Lewy bodies involves a shift in the synthesis as well as in the clearance of native αSyn, leading to more unfolded monomers that cannot be cleared. These monomers aggregate into oligomers, protofibrils, and insoluble fibrils that finally accumulate in Lewy bodies. These Lewy bodies-αSyn aggregations are believed to cause progressive dopaminergic neuron loss in the substantia nigra leading to PD motor impairment (1) (**Figure 1**, right panel).

In addition to the accumulation of neurotoxic forms of extracellular Aβ and intracellular αSyn, microglial activation in response to these aggregates drives NDD pathogenesis by activating the proinflammatory immune response (3). Microglial cells are CNS-resident macrophages with a plethora of functions, such as maintaining homeostasis in brain development, and they survey the parenchyma and react to damage, foreign and redundant particles. In response to a harmful stimulus such as brain injury or the presence of pathogens, microglial cells become activated and can now trigger both protective and harmful reactions. Particularly for NDDs, microglial cells become activated when triggered by the presence of amyloids, causing microglial cells to migrate to and surround these Aβ-plaques and Lewy bodies, followed by induction of the innate immune responses (**Figure 1**). Furthermore, amyloids activate receptors on microglial cells, causing a secretion of proinflammatory cytokines and chemokines. Additionally, after receptor activation, microglial cells engulf amyloids via a process called **phagocytosis** (3, 5). Whether phagocytosis is beneficial or harmful for disease progression is still under debate. In addition, loss of mitochondrial membrane potential and membrane-associated oxidative stress are also important in the pathogenesis of NDDs. They can cause neuronal excitotoxicity, which will contribute to neuronal death (9, 10). Both Aβ and αSyn bind to glutamate receptors on neurons and microglial cells (11-14). Glutamate transmission regulates cognition, learning, and memory. However, excessive glutamate can cause **excitotoxicity**, leading to cell death which plays an important role in AD and PD progression (15). Aβ and αSyn accumulations lead to mitochondrial dysfunction that causes excessive reactive oxygen species (ROS) formation. The resulting oxidative stress contributes to the progression of AD and PD (16). Accumulation of Aβ and αSyn, causing microglial activation, excessive ROS formation, and cellular toxicity, amongst others, are the main contributors to AD and PD progression.

Some treatments are available from which the mode of action is to slow disease progression, although their approval by the Food and Drug Administration (FDA) and European Medicine Agency (EMA) remains absent. For example, aducanumab, a disease-modifying drug to slow down AD pathogenesis by aiding in clearing plaques, recently got FDA approved, yet not EMA-

approved (17, 18). Since the beginning of 2023, Lecanemab, a new modifying drug to slow down AD pathogenesis by aiding in clearing plaques, was recently FDA and EMA-approved (19). For PD, there are only FDA/EMA-approved drugs targeting motor symptoms, like Levodopa, to replenish dopamine, yet there is no FDA-approved medication to slow disease progression (20). To address the fast-increasing aging population and, consequently, the acceleration and severity of NDDs, new and more potent therapeutic approaches that target the pathology of the disease are urgently needed. Nonetheless, additional research is needed to examine the complex development of NDDs to find therapeutics that slow disease progression. Here in this project, we aim to find a simple but applicable **research model to screen therapeutics** that might affect NDD progression. Developing such research models is challenging since *in vitro* models lack the organism's complexity and physiological growth conditions (21). Nonetheless, *in vivo* models fail to accurately predict clinical trial results due to the species-specific differences in neurobiology and physiology (22, 23). Recently, 3-dimensional (3D) neuronal organoids of human induced pluripotent stem cells (iPSCs) seem promising to overcome the *in vitro* and *in vivo* limitations. (22). In spite of that these models have several limitations as they are expensive, labor-intensive, and challenging to reproduce (23). In the future, it is predicted that these organoids will serve as an effective model for screening the efficacy of treatments.

Advancements in *in vitro* cell culturing models are required to make them reproducible and more applicable to the human body's complexity. A pivotal step in using *in vitro* models is the establishment of reliable assays to monitor NDD disease-specific readouts. **Our research goal** is to validate *in vitro* disease-induced cellular models of neuronal (SH-SY5Y) and microglial (HMC3) cell cultures that can be used as first-based screening of disease-modifying compounds for NDDs prior to screening in *in vivo* models. Therefore, in this research, we investigated if the *in vitro* AD-and PD-induced HMC3 and SH-SY5Y model can represent NDDs disease-specific readouts and thus can be used as an *in vitro* cell culture model for custom-based research. Our goal will be achieved by validating phagocytosis and cell viability on our models, as these readouts are the primary physiological readouts for NDDs. This research builds the foundation for developing a co-culture model in the next step of this research. This co-culture model will be the first neuronal-microglial cell model at InnoSer that will be commercially available for custom-based research to screen disease-modifying drugs for NDDs. This project will support pharmaceutical companies in the screening of NDD therapies with focus on reducing disease progression of AD and PD patients.

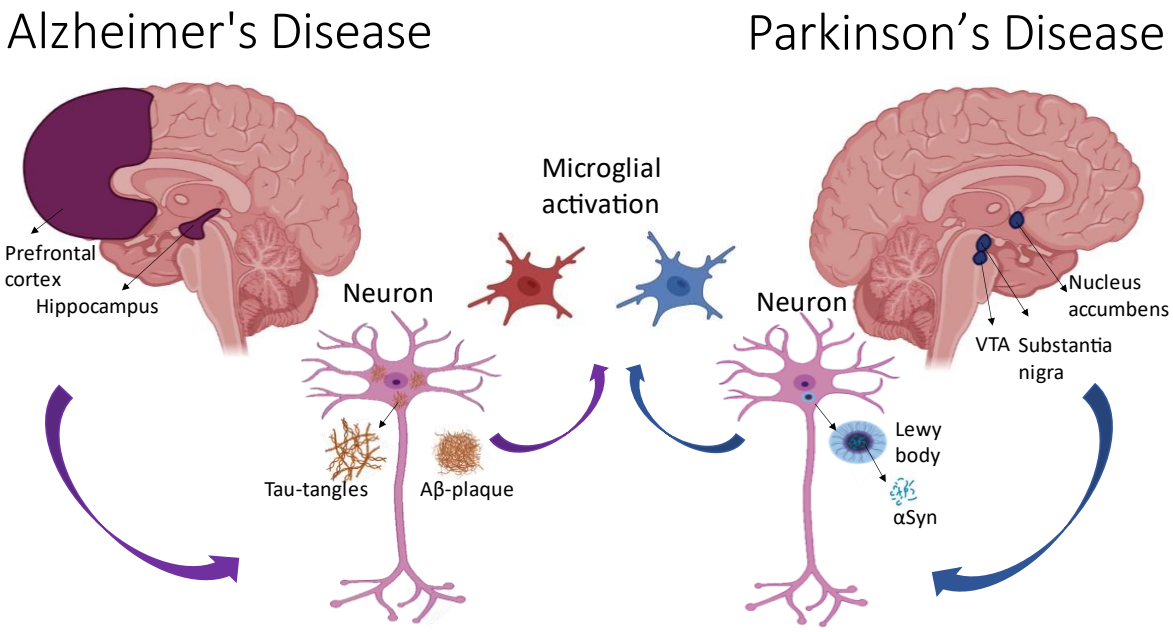

Figure 1: Overview of Alzheimer's Disease (left) and Parkinson's Disease (right) pathology. Created with BioRender.

EXPERIMENTAL PROCEDURES

Cell culture - Human neuroblastoma cells (SH-SY5Y, Cat. No. 94030304) were purchased from the European Collection of Authenticated cell cultures (ECACC), UK). The human microglia clone 3 cell line (HMC3, Cat. No. CRL 3304) was obtained from Creative Biolabs, (US). SH-SY5Y cells were cultured in Dulbecco's Modified Eagle's Medium with pyruvate (DMEMp+, Gibco, Cat. No. 41966029) supplemented with 10% Fetal Bovine Serum (FBS, Gibco Cat. No. 10438026) and 1% Penicillin/streptomycin (P/S, Gibco Cat. No. 15070063). Undifferentiated cells were grown to 80-90% confluency and seeded in well plates for further experiments. To start neuron-like differentiation cell seeding medium was changed to DMEM without pyruvate (DMEMp-, Gibco Cat. No. 41965039) supplemented with 5% FBS, 1% P/S, and 10 µM Retinoic acid (RA, Sigma-Aldrich, Cat. No. R2625) further mentioned as DF1 medium. Hereafter on day 4, the medium was replaced with neurobasal medium (Gibco Cat. No. 12349015) supplemented with 2 mM L-Glutamine (Gibco Cat. No. 25030024), 10x N-2 Supplement (Gibco Cat. No. 17502048), 1 µg/ml Human Bone Derived Neurotrophic factor (hBNDF, Invitrogen Cat. No. RP-8642), and 1% P/S further mentioned as DF2 medium. Cells remained in this medium until the end of differentiation at day 7. Whereafter they are ready to use for experiments. HCM3 cells were cultured in DMEMp- supplemented with 10% FBS and 1% P/S. HMC3 cells were grown to 80-90% confluency and seeded in well plates for further experiments. All cell cultures were cultured in a humidified atmosphere at 37 °C and 5% CO_2. Cells were between passage 4-15 for all experiments in this study.

HCM3 phagocytosis – *Human Synthetic* Amyloid Beta 1-42 Pre-formed Fibrils (fAβ, StressMarq Biosciences, Cat. No. SPR-487), and Human Recombinant Alpha-Synuclein Pre-formed Fibrils (fαSyn, StressMarq Biosciences, Cat. No. SPR-322) were used to mimic AD and PD models. For phagocytosis, these fibrils were labeled with pHrodo red (f^{pH}) (Thermofisher Scientific, Cat. No. P36600) based on the FUJIFILM protocol of labeling amyloid Beta with pHrodo red without performing the aggregation step (24). Hereafter, fibrils were sonicated at RT for 2x4 min, 9 cycli at 80% power. Cells were seeded at 5000 cells per well in a 96-well plate for approximately 16 h prior to the start of the experiment. Treatment with $fA\beta^{pH}$ or $f\alpha Syn^{pH}$ was performed in DMEMp-supplemented with 2% FBS and 1% P/S. To validate the efficacy of aducanumab as a control for the AD phagocytosis model, HMC3 cells were treated with aducanumab (ProteoGenix, Cat. No. PX-TA1335) concentrations of 0.0 - 0.01 - 0.1 - 0.5 µg/ml together with $fA\beta^{pH}$ at concentrations of 0.0 -1.0 - 2.0 - 5.0 µM in a total of 100 µl fresh medium per well. To represent PD, HMC3 cells were treated with $f\alpha Syn^{pH}$ at concentrations of 0.0 - 0.5 – 1.0 – 2.5 µM in a total of 100 µl fresh medium. At least two technical replicates were used for each treatment condition. The plates were immediately placed in an IncuCyte S3 Live-Cell Analysis System (Essen BioScience), and 1 image per well was captured at 1 h time intervals for 72 h at an exposure time of 600 msec. with a 10x objective. The fluorescence intensity, cell confluence, and integrated fluorescence intensity data were obtained and analyzed using the GraphPad Prism software. The phagocytic capacity of the pHrodo labeled fibrils was measured as the Relative phagocytosis Integrated Intensity (RCUx μm^2/Image), defined as a normalized value relative to the initial fluorescent intensity at a specific time point (t) subtracted by the initial fluorescent intensity at time point zero (t=0).

Cell viability – Cell viability was performed using 3-(4,5-Dimethylthiazol-2-yl)-2,5-diphenyltetrazolium bromide (MTT, Sigma-Aldrich, Cat. No. 11465007001) according to the manufacturer's instructions. In brief, HMC3 cells were seeded at different densities 2500 – 5000 - 10000 - 15000 - 20000 - 25000 - 30000 and 35000 cells per well in a 96-well plate to determine the optimal density for further HMC3 MTT experiments. Based on density optimization, HMC3 cells were seeded at a density of 10000 cells/well, followed by incubation for 16 h before treatment. For treatment with L-Glutamate (ThermoFisher Scientific, Gibco Cat. No. 25030024), freshly prepared L-glutamate was used in all experiments, and it was further dissolved in a culture medium to obtain the required concentrations. For analyzing the toxic effects of L-glutamate at different concentrations, the cells were treated with 0 – 10 – 20 – 30 - 40 and 60 mM of L-

glutamate for 24 h. For treatment with fibrils, fAβ and Human Recombinant Tau (K18, P301L) Pre-formed Fibrils (fTau, StressMarq Biosciences, Cat. No. SPR-330) were used to mimic AD models, and fαSyn was used to mimic the PD model. The toxic effect of fibrils was assessed by treatment with 0 – 10 or 20 µM fAβ, fTau or fαSyn. Fibrils were sonicated as described previously. SH-SY5Y cells were seeded at different densities 1600 - 3200 - 6400 – 9600 - 12800 - 16000 - 19200 and 22400 cells per well in a 96-well plate to determine the optimal density for further SH-SY5Y MTT experiments. Based on density optimization, SH-SY5Y cells were seeded at a density of 6400 cells/well followed by differentiation, as mentioned earlier. For analyzing the toxic effects of L-glutamate, fAβ, fTau, and fαSyn on SH-SY5Y cells the same concentrations mentioned for HMC3 cells were used. 20 h after the start of the treatment, MTT labeling reagent (final concentration 0.5 mg/ml) was added to each well and incubated for 4 h at 37 °C in a humidified incubator. After incubation, MTT solubilization solution was added to each well and placed back in the incubator overnight. The next day, the absorbance was measured at 560 nm using a microplate reader (GloMax, Promega). The untreated cells were used as control and considered with 100% cell viability for further analysis.
To select the medium for the co-culture experiments. The ReadyProbe cell viability imaging Kit (Blue/Red) (Invitrogen, Cat. No. R37610) was used to stain all cells with NucBlue and dead cells with Propidium Iodide. 2 drops of each stain were added per ml medium. Cells were incubated for 15 min before cell scoring was done with ImageXpress Micro 4 (Image Express Micro 4, Molecular Devices).

Immunofluorescence staining – IF staining's were performed to determine the differentiation of SH-SY5Y cells and to establish the co-culture of HMC3 and SH-SY5Y cells. 12 mm glass cover glasses were coated with 0.01% laminin (Sigma-Aldrich, Cat. No. L2020-1MG) for at least 2 h before seeding. SH-SY5Y cells were seeded at 19000 cells/well in a 24-well plate and differentiated. On day 7, a 1/5 ratio of HMC3 cells was added to SH-SY5Y cells in DF2 medium. After seeding (and differentiation), cells were washed with 1x Phosphate buffered saline (PBS, Capricorn Scientific, Cat. No. PBS-1A) and fixed with 4% paraformaldehyde (PFA, VWR chemicals Cat. No. 19B214202) for at least 10 min at room temperature (RT). Afterwards, cells were gently washed 3 times with 1x PBS followed by permeabilization with 0.1% Triton X-100 in 1x PBS buffer (PBS-T, Sigma-Aldrich, Cat. No. STBJ4510) for 10 min at RT. Cells were blocked for 60 min at RT with PBS-T supplemented with 5% donkey serum (Abcam Cat. No. AB7475), followed by overnight primary antibody incubation at 4 °C. The following primary antibodies were used: monoclonal anti-beta Tubulin III AB (βTubIII, mouse, 1:500, Sigma, Cat. No. T8578) and anti-microtubule-associated protein 2 AB (MAP2, chicken, 1:500, Abcam, Cat. No. ab92434) to visualize mature SH-SY5Y cells. To visualize HMC3 cells, an anti-ionized calcium-binding adaptor molecule 1 AB (Iba1, rabbit, 1:250, Abcam, Cat. No. ab178846) was used. The next day, cells were washed 3 times with 1x PBS followed by incubation with the secondary antibodies coupled to Alexa Fluor 594 (βTubIII, Donkey, anti-mouse, 1:500, Abcam, Cat. No. ab150108), Fitch (MAP2, Donkey, anti-chicken, 1:30, Abcam, Cat. No. ab63507) and Alexa Fluor 488 (Iba1, Donkey, Anti-rabbit, 1:500, Abcam, Cat. No. ab150073) for 1 h at RT. Simultaneously with secondary antibody incubation, NucBlue (Invitrogen Ready Probes, Cat. No. R37606) was added to stain all cell nuclei. Cells were washed with 1x PBS at least 3 times and subsequently imaged with the ImageXpress Micro 4.

Statistical analysis - Statistical analysis and graphs were produced using Prism 9 (GraphPad Software 9.5.1). Data distributions were assessed for normality (Shapiro-Wilk). In case these assumptions were met for all groups, a One-Way or Two-Way ANOVA was performed. When the data distribution of at least one group was non-Gaussian, a non-parametric test such as the multiple Mann-Whitney U test or Kruskal-Wallis test was used. The reader is referred to the figure legends for details about the sample size (n) and specific statistical analysis. Graphs represent the mean and SEM. p-values smaller than p**** <0.0001, p*** 0.001, p** 0.005 and p*0.05 were considered significant.

RESULTS

SH-SY5Y neuroblast cells were successfully differentiated into mature neuronal-like cells.

BF images were collected to identify the morphology and condition of the cells throughout the differentiation process (**Figure 2**). Additionally, specific neuronal markers were stained to determine mature-like neurons (25). Anti-Microtubule-associated protein 2 (MAP2) is used as a mature, specific marker for neuronal-like cells, and it marks the neuronal dendrites and soma but not axons (**Figure 3**) (26). Anti-Beta III Tubulin (βTubIII) is used as a specific marker for neuronal differentiation, and it marks cell bodies, dendrites, and axonal terminations (**Figure 3**) (27, 28). Undifferentiated SH-SY5Y neuroblastoma cells on differentiation day 1, prior to the introduction of DF 1 medium, demonstrate a large, flat, epithelial-like phenotype with numerous short, stubby processes extending outward and dispersed over the well (**Figure 2A**, **B**, DF Day 1). Following 4 days of differentiation before changing to DF2 medium, the early SH-SY5Y differentiated cells demonstrate a large fat body, with more, longer processes extending outward (**Figure 2A, B** DF Day 4, blue arrow). After 7 days of differentiation, the SH-SY5Y cells demonstrate a more mature neuron-like phenotype with several neurite projections connecting with surrounding cells. Hereby, cells appear more in clusters (**Figure 2A**, **B** DF Day 7 and DF Day 9, green arrows). On the immunofluorescence images, an increase in MAP2 and βTubIII (**Figure 3**) was seen over the 9 days of differentiation, indicating neurite outgrowth formation.

Taken together, the neuronal characteristics of differentiated SH-SY5Y cells were demonstrated.

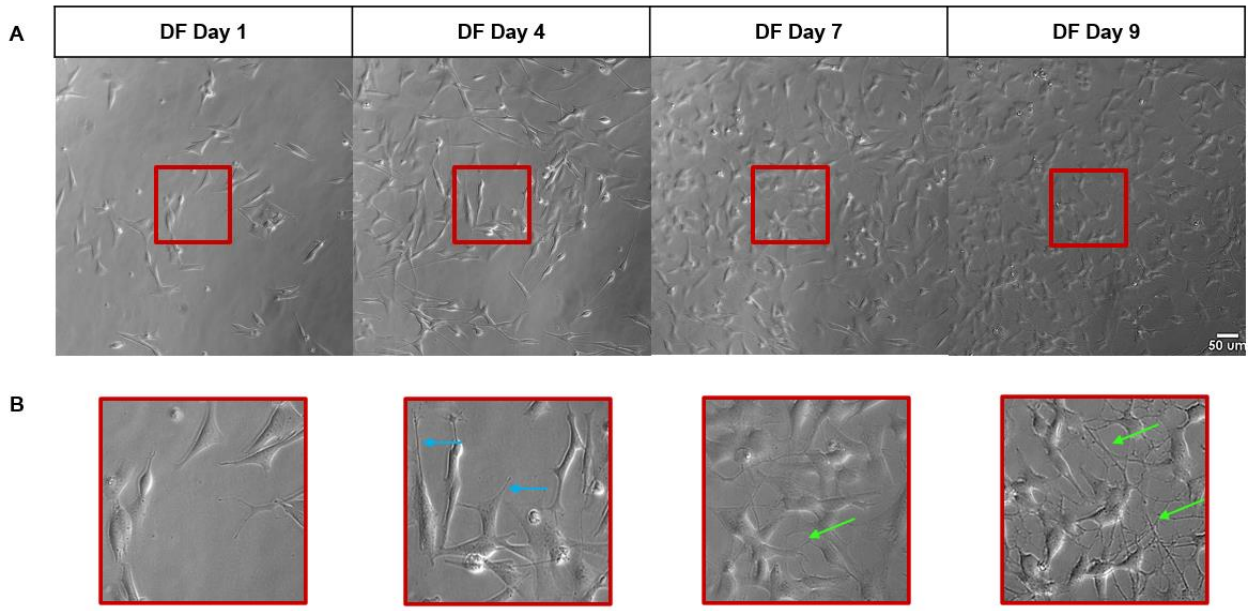

Figure 2: Morphological difference between undifferentiated and differentiated SH-SY5Y cells. A SH-SY5Y cells on DF Day 1 are singly dispersed over the well and show a flat phenotype with few and short projections, while on DF day 4, the cells have a more mature phenotype with more, longer projections (blue arrow) and start to form clusters with surrounding cells. After DF day 7, SH-SY5Y cells represent a mature phenotype with extensive and elongated neuritis outgrowths (green arrows) and are more situated in clusters of cells. **B** Magnification of a selected area (red box) of the images respectively in A. Images were obtained at 20X magnification using the ImageXpress Micro 4. Scale bar, 50 µm.

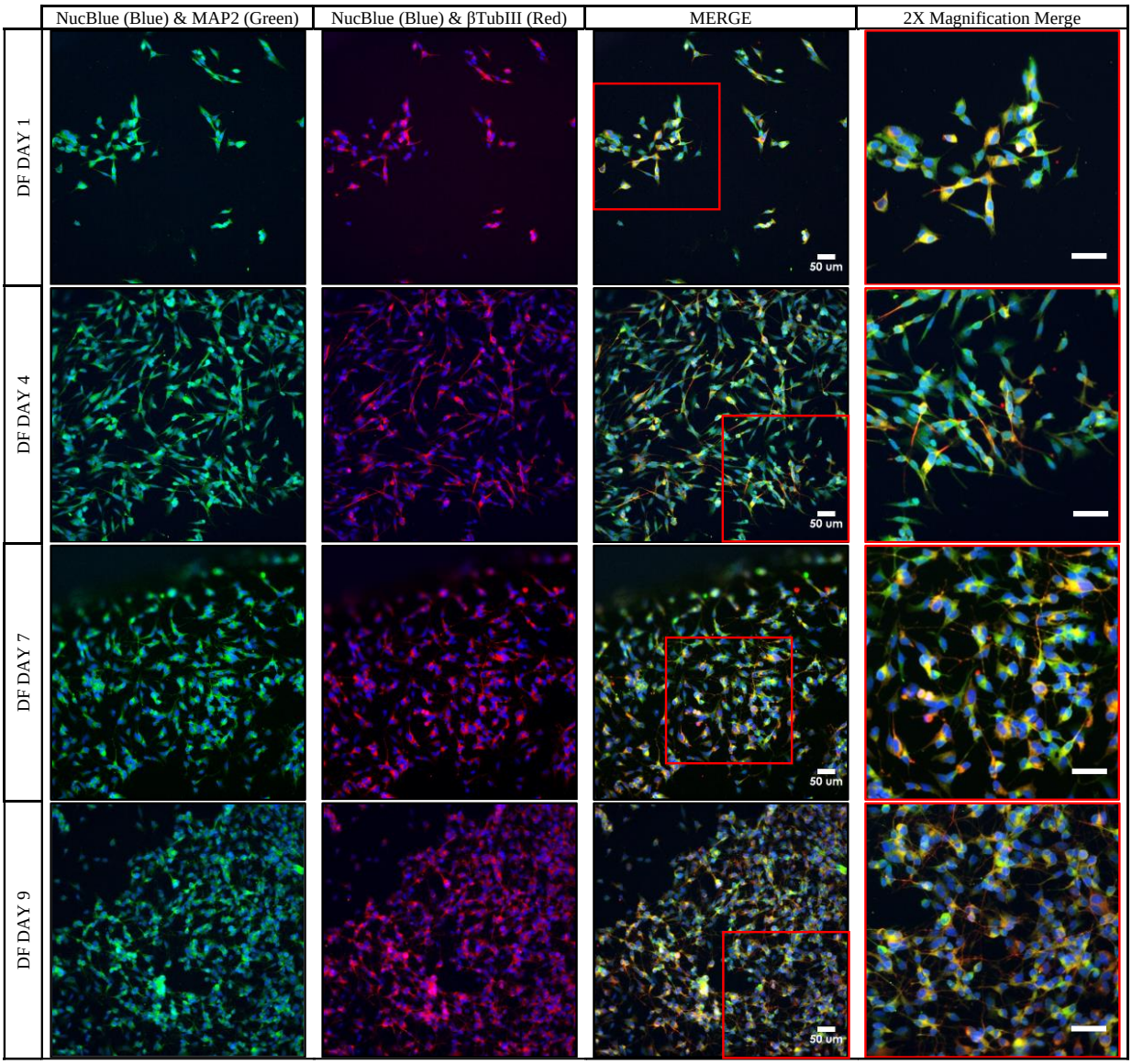

Figure 3: After 7 days, SH-SY5Y cells were differentiated into mature-like neurons. MAP2 (Red) labels mature neuronal-like cells. It labels the neuronal dendrites and soma but not the axons. βTubIII (Green) is a specific marker for neuronal differentiation and stains neuronal cell bodies, dendrites, and axonal terminations. NucBlue (Blue) dyes the nuclei of cells. The right panel shows the corresponding 2X magnification of a selected area (Red square) on the merged image. Images were obtained at 20X magnification using the ImageXpress Micro 4. Scale bar, 50 µm.

The induction of Alzheimer's and Parkinson's disease in the cellular models significantly increased phagocytosis.

We tested the phagocytic capacity of HMC3 cells in an AD and PD model. To represent each disease, HMC3 cells were treated either with fAβ to mimic AD or fαSyn to mimic PD. To assess the phagocytic capacity in real-time of live microglial cells, HMC3 cells were either treated with pHrodo red labeled fAβ (fAβ^{pH}) or with pHrodo red labeled fαSyn (fαSyn^{pH}). Live-cell images were acquired every 60 min for 72 h to measure the fluorescent intensity of the engulfed fibrils. Phagocytic capacity was quantified as the relative phagocytosis integrated intensity, *i.e.*, fluorescence compared to initial time (t=0) fluorescence. We observed internalization and increased phagocytosis of fAβ^{pH} (**Figure 4A**) and fαSyn^{pH} (**Figure S1A**) by HMC3 cells. In particular, a slow yet significant increase in phagocytic capacity after 56 h treatment with 2.5 µM fαSyn^{pH} was observed (**Figure S1B**). In comparison, there was a slow yet significant increase in phagocytic capacity after 52 h treatment with 2.0 µM fAβ^{pH} **(Figure 4B**). Additionally, treatment with 0.1 µg/ml Aducanumab significantly increased phagocytosis of fAβ^{pH} after 52 h compared to microglial cells solely in the presence of fAβ^{pH} (**Figure 4C**). Overall, our data shows that the phagocytic capacity significantly increased for HMC3 cells after treatment with fAβ or fαSyn.

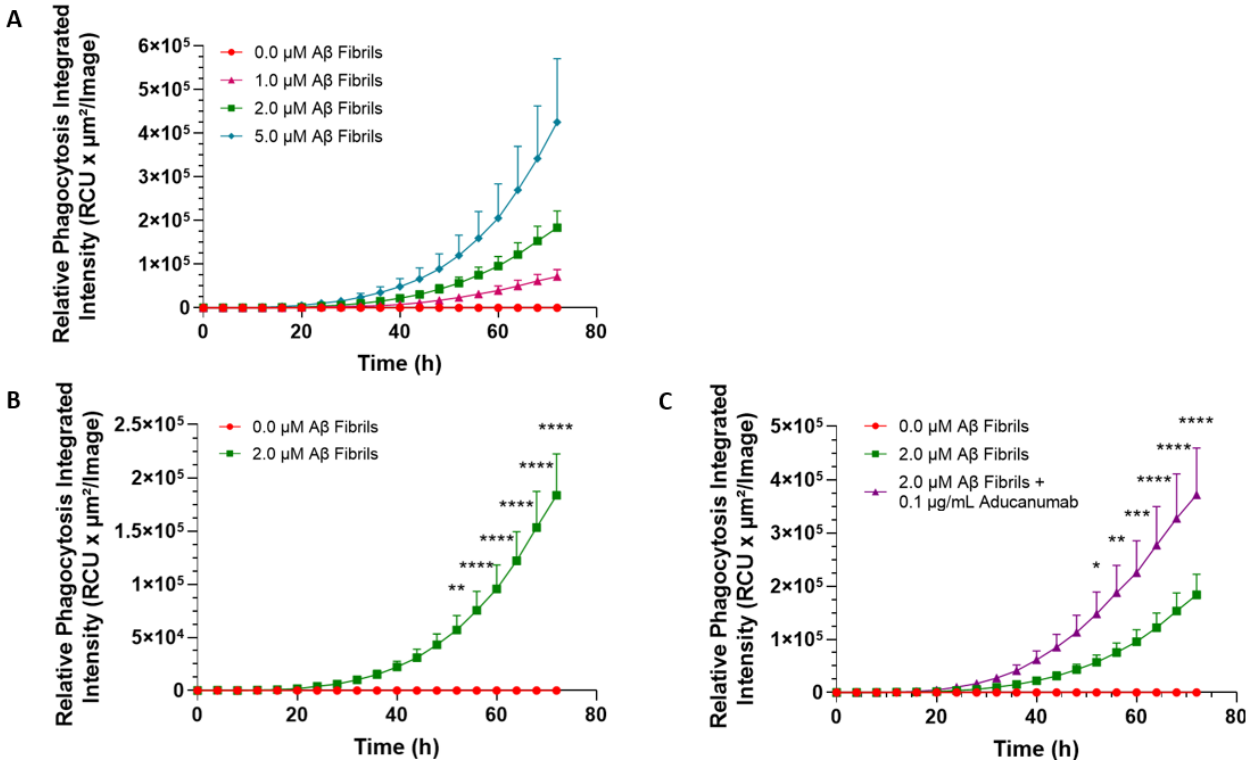

Figure 4: Aducanumab significantly increases phagocytosis in an Alzheimer's model. A HMC3 cells phagocytosis fAβ^{pH}. **B** HMC3 cells significantly phagocytose fAβ^{pH} after 52 h (**p=0.005) and after 56 h compared to baseline (0.0 µM fibrils) (**** p< 0.0001). **C** HMC3 cells significantly increase phagocytosis of the fAβ^{pH} model upon simultaneous treatment of 0.1 µg/ml Aducanumab compared to treatment with 2,0 µM fibrils alone (*p=0.05, ** p=0.005, ***p=0.001, ****p>0.0001). Data was obtained from IncuCyte S3 Live-Cell Analysis System. Phagocytic capacity was quantified as the relative phagocytosis integrated intensity, *i.e.*, fluorescence compared to initial time (t=0) fluorescence. Data points represent mean ±SEM of n=3 per condition. Two-Way ANOVA Dunnett's-multiple comparisons test.

Optimal seeding densities are required for cell viability measurements.

Cells were seeded at different densities to determine the ideal cell density for measuring cell viability with an MTT assay. Cell densities of 6400 and 9600 showed a near 100% cell viability for SH-SY5Y cells (**Figure 5A**), while optimal density for microglial cells, i.e., viability close to 100%, was 25000 and 30000 cells per well (**Figure 5B**). To confirm our selected densities, a pilot experiment using glutamate was performed (data not shown), indicating that a glutamate concentration range on 6400 SH-SY5Y cells/ well and 10000 HMC3 cells/well best represented the positive correlation of cell death with increasing glutamate concentrations. Therefore, the density of 6400 SH-SY5Y cells/well and 10000 HMC3 cells/well were used for further cell viability assays.

The induction of Alzheimer's and Parkinson's disease in the cellular models significantly decreased cell viability.

Following previous experiments, SH-SY5Y cells were seeded at 6400 cells/well and differentiated for 7 days, and HMC3 cells were seeded at 10000 cells/well for each experiment. Cell viability was preliminary measured with glutamate as this neurotransmitter can cause neurotoxicity in AD and PD (10). Glutamate excitotoxicity is a cell death mechanism triggered by excessive glutamate in neurons and microglial cells. Viability was measured 24 h after treatment with glutamate. After induction with different concentrations of glutamate, the MTT assay showed that cell viability was significantly decreased in SH-SY5Y (**Figure 6A**) and HCM3 (**Figure 6B**) cells in a concentration-dependent manner.

Cell viability of the AD model was determined using treatment of fAβ. After incubation with fAβ, cell viability was significantly decreased in SH-SY5Y (**Figure 6C)** and HMC3 (**Figure 6D**) cells. Preliminary data showed that Tau fibrils significantly decrease cell viability in our AD model in SH-SY5Y cells (**Figure S2A**) and a positive decrease in cell viability in HMC3 cells (**Figure S2B**). Cell viability of the PD model was determined using induction of fαSyn. Data showed that cell viability was significantly decreased after stimulation with fαSyn in SH-SY5Y (**Figure S2C**) and HMC3 (**Figure S2D**) cells. Taken together, increasing concentrations of fibrils resulted in a concentration depended decreased cell viability.

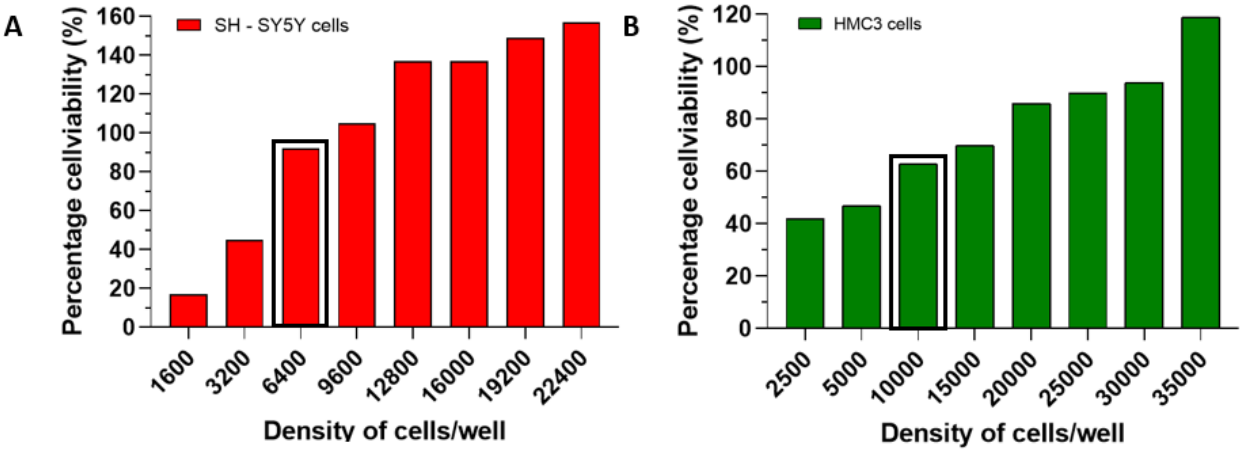

Figure 5: Lower seeding densities are suitable for cell viability measurement with MTT. The optimal cell density required **A** 6 400 cells/well for SH-SY5Y (black box) and **B** 10 000 cells/well for HMC3 (black box). Data was obtained with MTT assay measured on a GloMax microplate reader.

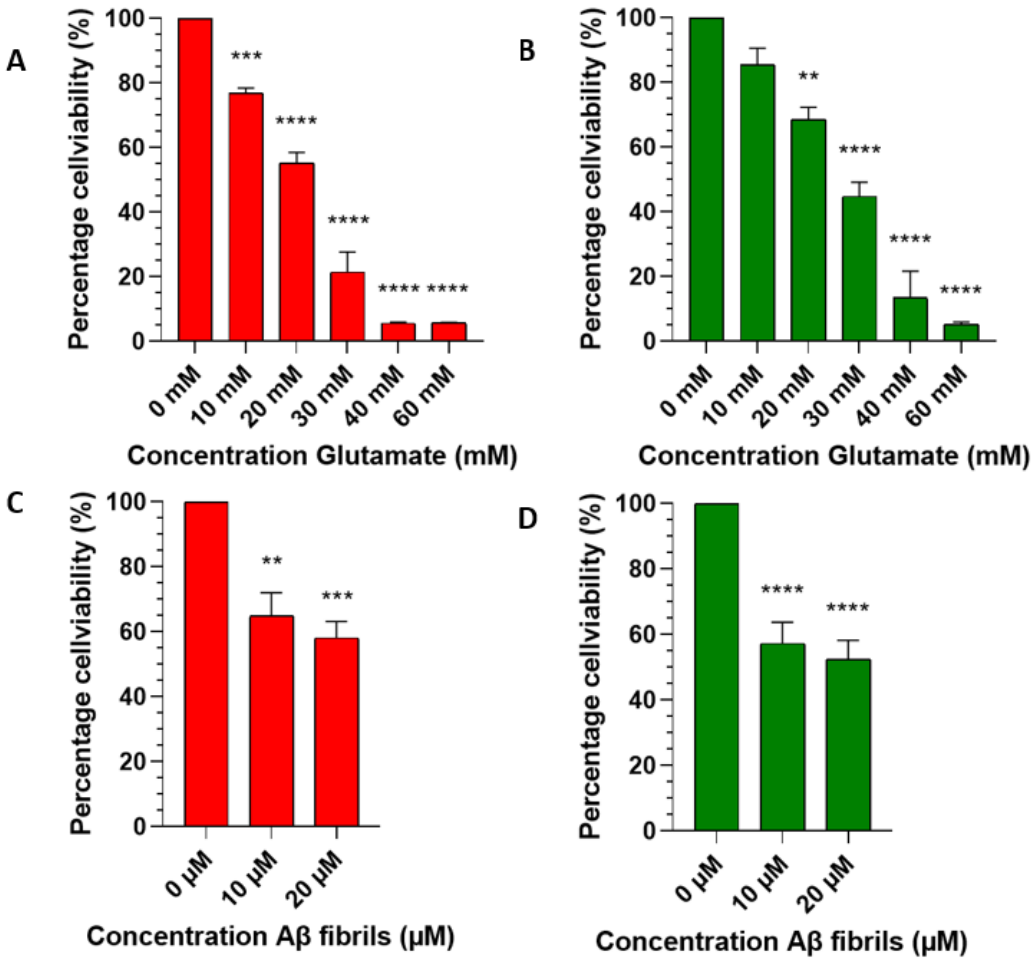

Figure 6: Cell viability decreased after incubation with glutamate or pre-formed Aβ fibrils. Glutamate treatment significantly decreases cell viability of **A** SH-SY5Y cells and **B** HMC3 cells. Aβ fibril treatment significantly decreases cell viability of **C** SH-SY5Y cells and **D** HMC3 cells. Data was obtained with MTT assay measured on a GloMax microplate reader. Each column represents mean±SEM of n=4 per condition. Asterisks indicate statistically significant differences compared to control (0 µM) (****p <0.0001, ***p<0.001, **p=0.005 and *p=0.05), One-Way ANOVA with Dunnett's multiple comparisons test.

HMC3 cells are viable and phagocytose in DF2 medium.

The co-culture medium needed to be selected as the SH-SY5Y and HMC3 cells were cultured in different mediums. Different mediums were evaluated, and the DF2 medium appeared the most suitable (data not shown). As SH-SY5Y cells do not phagocytose, only HMC3 cell viability and phagocytic capacity were evaluated when seeded in DF2 medium. First, cell viability of HMC3 cells was evaluated for 72 h in DF2 medium with ReadyPobe cell viability staining every 24 h in their expansion medium compared to DF2 medium (**Figure 7A**). Cell scoring was performed based on cell scoring program with ImageXpress Micro 4 that calculated the positive cells for NucBlue (total number of cells) and subtracted them by positive cells for propidium iodide (number of death cells). The result showed a mild decrease in cell viability, but the difference was not significant between the HMC3 in their expansion medium or DF2 over 72 h. Sequentially a trial to evaluate the phagocytic capacity of HMC3 in DF2 medium was conducted (**Figure 7B**). Data showed that HMC3 cells exhibit phagocytic capacity of $fA\beta^{pH}$ in DF2 medium. These data validated that DF2 medium was a viable and functional medium for future co-culture experiments.

Hereafter, neuronal and microglial cell characteristics in the co-culture were visualized by immunofluorescence detection of classical markers. βTubIII was used to visualize fully

differentiated SH-SY5Y cells (**Figure 8A**), and anti-ionized calcium binding adaptor molecule 1 (Iba1) was used to visualize HMC3 cells (**Figure 8B**). However, preliminary co-culture data showed that Iba1 was positive for SH-SY5Y cells (**Figure S3**).

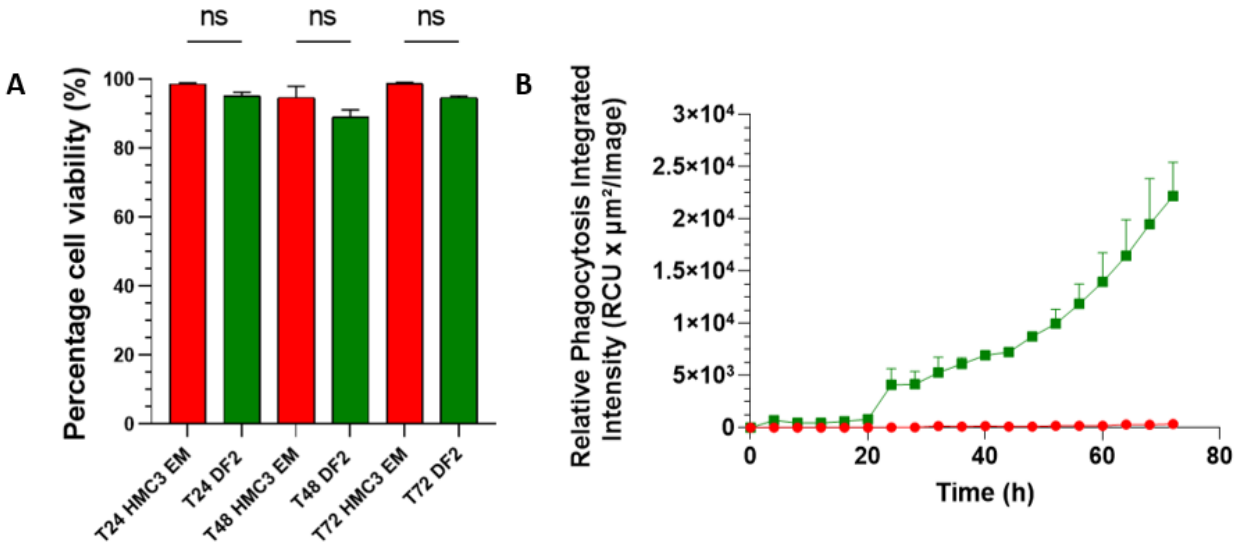

Figure 7: HMC3 cells were viable and functional in DF2 medium. A Cell viability of HMC3 cells was not significantly decreased in DF2 medium compared to HMC3 expansion medium (EM). Data was obtained with ReadyProbe cell viability staining imaged, and cell scored with ImageXxpress Micro 4. Each column represents mean±SEM; data showed no significance with a Two-Way ANOVA Dunnett's multiple comparisons test. **B** HMC3 cells phagocytose fAβ^{pH} in DF2 medium. Data was obtained from IncuCyte S3 Live-Cell Analysis System. Phagocytic capacity was quantified as the relative phagocytosis integrated intensity, *i.e.*, fluorescence compared to initial time (t=0) fluorescence. Data points represent mean ±SEM of n=1. Multiple Mann-Whitney test.

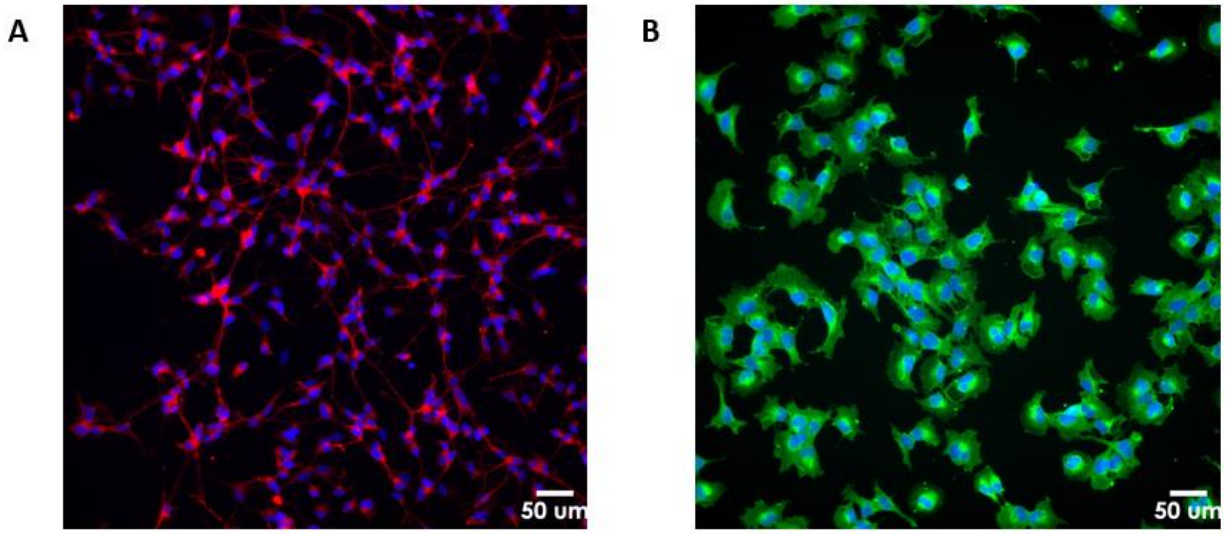

Figure 8: Positive staining for βTubIII on SH-SY5Y and Iba1 on HMC3 cells. A βTubIII (Red) stains neuronal cell bodies, dendrites, and axonal terminations in fully differentiated SH-SY5Y cells. **B** Iba1 (Green) stains the calcium-binding protein in HMC3 cells. Images were obtained at 20X magnification using the ImageXpress Micro 4. Scale bar, 50 µm.

DISCUSSION

Due to population aging, NDDs will be the top two causes of mortality among the elderly in 20–30 years. Currently, most therapies focus on relieving symptoms rather than preventing disease progression. AD and PD are the two most common NDDs where fibrils are the main cause of disease progression. AD and PD drug development is slowed due to a lack of in vitro reproducible models that imitate human complexity that can screen disease-modifying therapies inexpensively, efficiently, and fast. Here, we investigated if our AD and PD models represented phagocytosis and decreased cell viability. Our *in vitro* AD and PD model represented phagocytosis of fibrils and decreased cell viability as readouts to screen disease-modifying drugs. These NDD models will evaluate AD and PD disease-modifying drugs cheaper, simpler, and faster before screening them in vivo. Our co-culture models for AD and PD were initiated yet not fully optimized, so future experiments are needed to validate phagocytosis and cell viability in our co-culture model.

Other models are used in neuronal research that better represent human complexity, such as primary neuronal cultures, induced pluripotent stem cells (iPSC) derived neurons, and organoids, nevertheless, we opted for SH-SY5Y cells, as this model is most frequently used for research purposes for AD and PD (29). The advantages of SH-SY5Y cells are that they are of human origin but obviate the ethical concerns associated with primary neurons and iPSC. They are easy to culture and maintain, which makes them cheaper and more used in research (29). As these cells are frequently used, they have a broad research application, additionally, they facilitate experimental reproducibility and global custom-based research. In this research, we differentiated SH-SY5Y cells to represent a more complex neuronal-like model of what may occur in neurons in vivo. The protocol described by M. Encinas (30) was used to optimize the differentiation of SH-SY5Y cells to yield highly viable, homogenous, differentiated neuronal-like cultures within 7 days. Differentiation was seen as successful when neurite outgrowths were established. For the first 4 days of differentiation, a medium with FBS starvation and the addition of retinoic acid (RA) to the cell culture media was used. RA is one of the most widely used and well-studied strategies for inducing differentiation in SH-SY5Y cells (25). RA is a vitamin A derivative that limits proliferation and promotes cellular differentiation (25). RA addition and serum deprivation initiate differentiation by increasing neurite branching and length (25). After 4 days in DF 1 medium, the SH-SY5Y cells showed early differentiation by protrusions of neurite outgrowth. For our DF2 medium, in which cells were differentiated until day 7 and kept until the end of experiments, a neurobasal-A medium minus phenol red was added with L-glutamate, N-2 supplement, and HBDNF. All medium factors, specifically this neurobasal medium, and HBDNF, were used to mature further and maintain the early differentiated cells (25).

Literature states 3 important steps for differentiation of SH-SY5Y cells, namely, addition of RA, serum deprivation, and addition of BDNF (25). Our results are in line with literature and show that indeed RA induction and gradual serum removal in accordance with BDNF addition contribute to the differentiation of neuron-like cells (25). Literature suggests that βTubIII and MAP2 are specific markers for neuronal differentiated cultures (26-28), therefore, the expression of these markers was investigated in our cultures. Our cells resembled the morphology as shown in literature (25). Additionally, immunofluorescent staining for βTubIII and MAP2 confirmed that the SH-SY5Y cells matured into neurons. It should be noted that differentiation of SH-SY5Y cells using RA can result in 3 types of mature neurons: dopaminergic, adrenergic, and cholinergic neurons (25). As a lot of controversy consists about the exact differentiation protocols for these particular of neurons, we state that in this research, we use mature neurons though did not distinguish between choleric neurons for AD (31) and dopaminergic neurons for PD (32).

Microglial cells are the first line defense in the CNS they protect the brain against harmful events such as, brain damage or foreign and redundant particles. Additionally, they can respond to a variety of environmental cues in order to maintain brain homeostasis. As a response to such harmful events microglial cells become activated, hereby mediating the inflammatory response by producing a cocktail of cytokines, chemokines or free radicals

such as nitric oxide, interleukin 1β (IL-1β) or tumor necrosis factor-α (TNF-α) (33). In case of NDD, like AD and PD, it is speculated that microglial cells get chronically activated resulting in an overproduction of these immune mediators thereby creating a neurotoxic environment (34, 35). However, later research also indicated a neuroprotective function for microglial cells after activation through the release of anti-inflammatory cytokines such as tumor growth factor-β (TGF-β) and brain derived neurotrophic factor (BDNF) (34). AD and PD is hallmarked by the presence of amyloid fibrils such as Aβ and αSyn. Aβ and αSyn can trigger microglial activation by stimulating microglial receptors such as toll-like receptor (TLR) 2, TLR4, complement receptors (CR) 1 and CR3, hereby not only inducing the release of proinflammatory cytokines and chemokines by microglial cells but also triggering phagocytosis, which is the process for clearing cellular debris, dying or death cells or pathogens (3, 5, 34-37). While non-pH-sensitive fluorophore conjugates of Aβ and αSyn have been extensively used to assess fibril phagocytosis in HMC3 cells (38-40), a pHrodo-based assay allows the conjugated fibrils only to be visible when phagocytosed (pH 4.5-5), making it ideal for live-cell imaging (41). Our results showed that the pHrodo labeled fAβ and fαSyn were successfully phagocytosed by HMC3 cells which establishes phagocytosis as a readout in our AD and PD model to screen phagocytosis-modifying drugs.

Treatments focusing on the increase of this phagocytotic capacity might contribute to ameliorating the prognosis of NDDs. For AD, aducanumab, a therapeutic agent that ameliorates the pathogenesis of AD, is on the market. Previous research showed that aducanumab binds to Aβ fibrils and clears amyloid plaques. However, if this clearance benefits the patients' symptoms is still under debate (42, 43). The mode of action of aducanumab is thought to be the increase of phagocytic capacity of microglial cells by stimulating the binding to Aβ-aggregates (44). Our model showed that aducanumab significantly increased fAβ phagocytosis, confirming previous research (44). Therefore, aducanumab can now be used as an internal control for testing other phagocytosis-directed AD therapeutics on this cellular model. For PD there is currently, no approved disease-modifying drug available, and therefore, we could not screen a reference therapeutic as a control for PD. Yet, our data showed that phagocytosis was increased after incubation with fαSyn. Overall, our results show the validation of the phagocytic capacity of HCM3 cells after treatment with fAβ and fαSyn allowing this cellular model to be used for the screening of other AD and PD fibril-modifying drugs.

Even though neuronal cell death is necessary for optimal nervous system development, neuronal loss inevitably results in functional decline, like memory loss and motor problems which underlies the progression of neurodegenerative diseases. This neuronal loss is often accompanied by microglial activation that can contribute to both neuronal and microglial death (45, 46). As cell death is another major factor in NDD progression we aimed to evaluate cell viability after treatment with fAβ and fαSyn to establish cell viability as a validated readout for screening other AD and PD disease-modifying drugs. Cell viability is sensitive to the addition of compounds and densities of seeding cells. Previous research showed that when cell density is too high, cells do not have enough space and neurites in the medium to proliferate, and they will eventually die, additionally, when fewer cells are seeded the effect of cell death can be covered by proliferation hereby cell death might be covered by the presence of new cells (47-49). Furthermore, in very low seeding densities, cells will not be able to complement from each other to grow as they need each other to proliferate and survive hereby inducing cell dead not solely caused by fibril treatment. Thus, to limit cell death due to not optimal seeding densities, a range of cell densities were tested for SH-SY5Y and HMC3 cells. The densities of 6400 SH-SY5Y cells/well and 10000 HMC3 cells/well were selected as optimal seeding densities for cell viability to limit the amount of cell death due to too low or too high seeding densities.

First, glutamate toxicity was evaluated on our model to optimize and validate the MTT assay. Glutamate, a major excitatory neurotransmitter in the CNS, plays an important role in AD and PD progression, as glutamate excitotoxicity leads to the death of neurons and glial cells (15, 50). Our results showed that cell viability was significantly decreased in SH-SY5Y and HCM3 cells after 24 h, with a positive correlation to increasing glutamate concentration. These results are in accordance with

previous research, showing that glutamate toxicity in neurons and glial cells decreased cell viability (51, 52). Our data showed that neurons are more susceptible to glutamate excitotoxicity compared to microglial cells. Although the exact reason why glutamate affects neurons more than microglial cells is difficult to state, as the research on the effects of glutamate excitotoxicity is more elaborate on neurons than microglial cells. However, it could be because microglial cells' reaction to glutamate is known to be either protective or harmful, depending on the glutamate receptors activated (14, 52), while the neuronal reaction to excessive glutamate is known to be toxic (51, 53-55).

Besides glutamate toxicity, fibrils contribute to NDDs progression by decreasing cell viability. Previous studies have demonstrated that Aβ, Tau, and αSyn caused neuronal and microglial cell death *in vitro*. Yet, the research was limited, and the effect of fTau and fαSyn on microglial cells remains unclear (56-61). Our research showed that SH-SY5Y and HMC3 cells treated with pre-formed fAβ, fTau, and fαSyn decreased their cell viability in a concentration-dependent manner. Preliminary data for fTau showed that cell death occurred similarly to fAβ fibrils, yet further experiments are needed to determine if this decrease is significant for HMC3 cells. Previous studies showed that Aβ, Tau, and αSyn fibrils are toxic for brain cells in AD and PD (62-65). Additionally, some literature states that Aβ fibrils and αSyn fibrils bind to glutamate receptors on microglial and neuronal cells resulting in neurotoxicity (11, 14, 66). Ultimately, Aβ, Tau, and αSyn fibrils cause excitotoxicity due to Ca^{2+} dysregulation, which induces cell death (65, 67).
These results validate our model for fAβ AD and fαSyn PD for cell viability as readout. However, future experiments are needed to validate cell viability in a fTau AD model.

Taken together we established differentiated SH-SY5Y cells, validated HMC3 phagocytosis, and decreased cell viability in our mono HMC3 and SH-SY5Y cell models. These validated AD and PD *in vitro* models can now be used to screen disease-modifying drugs or contribute to developing a co-culture model.

Establishing a co-culture of HMC3 and SH-SY5Y cells is the next step to increase complexity and consider microglial-neuron interactions in our model. Microglial cells are beneficial in diseases by clearing up unwanted substances, such as pathogens and dead cells. However, when this injury is chronic microglial cells release cytotoxic mediators that contribute to neuronal cell degeneration (63, 64). Since SH-SY5Y and HMC3 cells were cultured in different mediums, a co-culture medium was selected wherein SH-SY5Y and HMC3 cell viability and HMC3 phagocytic capacity was assessed. Our findings indicate that DF2 media is adequate for co-culture studies, as this was one of the differentiation media of SH-SY5Y cells and HMC3 cells showed only a mild loss in cell viability and phagocytosis of HMC3 cells.

Immunofluorescence staining's were performed on mono-cell cultures and co-cultures to visualize our co-culture and distinguish between SH-SY5Y and HMC3 cells in co-culture experiments. SH-SY5Y cells were visualized with a selective neuronal marker, βTubIII (27), and HMC3 cells with a selective microglial marker, Iba1 (49, 68), and HMC3 cells with a selective microglial marker, Iba1. Surprisingly, our co-culture trials showed that Iba1 is not a selective marker for microglial cells as the SH-SY5Y cells stained positive for Iba1, which contradicts research stating that Iba1 is a well-established specific marker for microglial cells activation (68). Upon microglial cell activation, Iba1 binds to a specific calcium-binding protein involved with membrane ruffling and phagocytosis. Iba1 should give a clear labelling of the cells' body and fine processes in activated microglial cells. Literature states that Iba1 is selective for only microglial cells and does not bind to other neuronal cells (44, 65-67). Technical errors in our optimalization approach could cause this false positive staining of Iba1 for SH-SY5Y cells. As an alternative the dilution concentration of Iba1 can be adapted, background noise can be limited by increasing the time and concentration of Triton in the permeabilization step. Besides the addition of other compound like tween or sodium dodecyl sulphate to the permeabilization step can decrease background noise. Using another blocking buffer in combination with donkey serum such as bovine serum albumin could limit unspecific binding of Iba1. In the future, to establish our co-culture, additional microglial markers in combination with a newly purchased Iba1 antibody will be used and

optimized to receive proper cell labeling. Such additional microglial markers are the purinergic receptor P2Y12 (P2RY12) and trans-membrane protein 119 (TMEM119) which label their name indicating receptor, in contrast to P2Y12R which is a well-studied receptor for ATP, the TMEM119 is a surface receptor with unknown function in the brain (69). Although additional markers are available there are concerns whether or not these markers are specific for (activated) microglial cells. There are concerns that these markers are non-specific for (activated) microglial cells as they are independent expressed on the surface of inactivated, activated microglial, and other cells (68-70). Even though we had a false positive staining for Iba1 in SH-SY5Y cells, these preliminary data will be the basis for establishing a co-culture of HMC3 and SH-SY5Y cells.

CONCLUSION

Phagocytosis and cell viability were established for our fAβ AD and fαSyn PD model, yet more research is needed to establish a fTau AD model. The validated models can directly be implemented in custom-based research for these two readouts. In the future other disease-specific readouts might be validated, such as ROS production and aggregation of fibrils. These data will contribute to ultimately establishing a HMC3-SH-SY5Y co-culture.

In conclusion, our AD and PD cell culture model represent phagocytosis and cell viability as readouts to screen disease-modifying drugs. Although, more research needs to be conducted to establish a co-culture model relevant to study the effect of disease-modifying drugs on microglial-neuron interactions our cellular models validated in this research provide a basis for investigating AD and PD disease-specific readouts upon administration of disease-modifying drugs.

Acknowledgments – A.L. is grateful to the Neurology and Cardiometabolic Diseases research group at Innoser Diepenbeek to allow her to do her Senior master internship. A.L. would like to specifically thank J.B. and TvN for the opportunity to let her work in their team. A.L. is grateful for all the opportunities she got during her senior master's internship and for the support she was given to work independently. Lastly, A.L. would like to thank all who have taken the time to explain and transfer their knowledge.

Author contributions – – J.B. and TvN. conceived and designed this study. A.L. performed the experiments and data analysis. A.L. wrote the paper. J.B. and TvN. revised and approved the final paper.

REFERENCES

1. Salahuddin P, Fatima MT, Uversky VN, Khan RH, Islam Z, Furkan M. The role of amyloids in Alzheimer's and Parkinson's diseases. Int J Biol Macromol. 2021;190:44-55.
2. Duraes F, Pinto M, Sousa E. Old Drugs as New Treatments for Neurodegenerative Diseases. Pharmaceuticals (Basel). 2018;11(2).
3. Simpson DSA, Oliver PL. ROS Generation in Microglia: Understanding Oxidative Stress and Inflammation in Neurodegenerative Disease. Antioxidants (Basel). 2020;9(8).
4. Alzheimer's and Dementia. Alzheimer's association.
5. Tiwari S, Atluri V, Kaushik A, Yndart A, Nair M. Alzheimer's disease: pathogenesis, diagnostics, and therapeutics. Int J Nanomedicine. 2019;14:5541-54.
6. Jankowsky JL, Zheng H. Practical considerations for choosing a mouse model of Alzheimer's disease. Mol Neurodegener. 2017;12(1):89.
7. Hur JY. gamma-Secretase in Alzheimer's disease. Exp Mol Med. 2022;54(4):433-46.
8. Get informed about Parkinson's disease with these key numbers. Parkinson's Foundation.
9. Mattson MP. Glutamate and neurotrophic factors in neuronal plasticity and disease. Ann N Y Acad Sci. 2008;1144:97-112.
10. Dong XX, Wang Y, Qin ZH. Molecular mechanisms of excitotoxicity and their relevance to pathogenesis of neurodegenerative diseases. Acta Pharmacol Sin. 2009;30(4):379-87.

11. Trudler D, Sanz-Blasco S, Eisele YS, Ghatak S, Bodhinathan K, Akhtar MW, et al. alpha-Synuclein Oligomers Induce Glutamate Release from Astrocytes and Excessive Extrasynaptic NMDAR Activity in Neurons, Thus Contributing to Synapse Loss. J Neurosci. 2021;41(10):2264-73.
12. Danysz W, Parsons CG. Alzheimer's disease, beta-amyloid, glutamate, NMDA receptors and memantine--searching for the connections. Br J Pharmacol. 2012;167(2):324-52.
13. Revett TJ, Baker GB, Jhamandas J, Kar S. Glutamate system, amyloid ss peptides and tau protein: functional interrelationships and relevance to Alzheimer disease pathology. J Psychiatry Neurosci. 2013;38(1):6-23.
14. Liu H, Leak RK, Hu X. Neurotransmitter receptors on microglia. Stroke Vasc Neurol. 2016;1(2):52-8.
15. Wang R, Reddy PH. Role of Glutamate and NMDA Receptors in Alzheimer's Disease. J Alzheimers Dis. 2017;57(4):1041-8.
16. Singh A, Kukreti R, Saso L, Kukreti S. Oxidative Stress: A Key Modulator in Neurodegenerative Diseases. Molecules. 2019;24(8).
17. Mortada I, Farah R, Nabha S, Ojcius DM, Fares Y, Almawi WY, et al. Immunotherapies for Neurodegenerative Diseases. Front Neurol. 2021;12:654739.
18. Europe A. European Medicines Agency rejects marketing authorisation application for aducanumab. Alzheimer Europe. 2021.
19. MARKETING AUTHORIZATION APPLICATION FOR LECANEMAB AS TREATMENT FOR EARLY ALZHEIMER'S DISEASE ACCEPTED BY EUROPEAN MEDICINES AGENCY. Eisai Global. 2023.
20. Parkinson's Disease: Causes, Symptoms, and Treatments. NIH National Institute on Aging. 2022.
21. Sakolish CM, Esch MB, Hickman JJ, Shuler ML, Mahler GJ. Modeling Barrier Tissues In Vitro: Methods, Achievements, and Challenges. EBioMedicine. 2016;5:30-9.
22. Linsley JW, Reisine T, Finkbeiner S. Cell death assays for neurodegenerative disease drug discovery. Expert Opin Drug Discov. 2019;14(9):901-13.
23. Jensen C, Teng Y. Is It Time to Start Transitioning From 2D to 3D Cell Culture? Front Mol Biosci. 2020;7:33.
24. FUJIFILM. Labeling Amyloid Beta with pHrodo Red 2019.
25. Kovalevich J, Langford D. Considerations for the use of SH-SY5Y neuroblastoma cells in neurobiology. Methods Mol Biol. 2013;1078:9-21.
26. Shipley MM, Mangold CA, Szpara ML. Differentiation of the SH-SY5Y Human Neuroblastoma Cell Line. J Vis Exp. 2016(108):53193.
27. Geisert EE, Jr., Frankfurter A. The neuronal response to injury as visualized by immunostaining of class III beta-tubulin in the rat. Neurosci Lett. 1989;102(2-3):137-41.
28. Filograna R, Civiero L, Ferrari V, Codolo G, Greggio E, Bubacco L, et al. Analysis of the Catecholaminergic Phenotype in Human SH-SY5Y and BE(2)-M17 Neuroblastoma Cell Lines upon Differentiation. PLoS One. 2015;10(8):e0136769.
29. Hoffmann LF, Martins A, Majolo F, Contini V, Laufer S, Goettert MI. Neural regeneration research model to be explored: SH-SY5Y human neuroblastoma cells. Neural Regen Res. 2023;18(6):1265-6.
30. Encinas M, Iglesias M, Liu Y, Wang H, Muhaisen A, Cena V, et al. Sequential treatment of SH-SY5Y cells with retinoic acid and brain-derived neurotrophic factor gives rise to fully differentiated, neurotrophic factor-dependent, human neuron-like cells. J Neurochem. 2000;75(3):991-1003.
31. de Medeiros LM, De Bastiani MA, Rico EP, Schonhofen P, Pfaffenseller B, Wollenhaupt-Aguiar B, et al. Cholinergic Differentiation of Human Neuroblastoma SH-SY5Y Cell Line and Its Potential Use as an In vitro Model for Alzheimer's Disease Studies. Mol Neurobiol. 2019;56(11):7355-67.
32. Xicoy H, Wieringa B, Martens GJ. The SH-SY5Y cell line in Parkinson's disease research: a systematic review. Mol Neurodegener. 2017;12(1):10.
33. Muzio L, Viotti A, Martino G. Microglia in Neuroinflammation and Neurodegeneration: From Understanding to Therapy. Front Neurosci. 2021;15:742065.

34. Bachiller S, Jimenez-Ferrer I, Paulus A, Yang Y, Swanberg M, Deierborg T, et al. Microglia in Neurological Diseases: A Road Map to Brain-Disease Dependent-Inflammatory Response. Front Cell Neurosci. 2018;12:488.
35. Colonna M, Butovsky O. Microglia Function in the Central Nervous System During Health and Neurodegeneration. Annu Rev Immunol. 2017;35:441-68.
36. Doens D, Fernandez PL. Microglia receptors and their implications in the response to amyloid beta for Alzheimer's disease pathogenesis. J Neuroinflammation. 2014;11:48.
37. Ho MS. Microglia in Parkinson's Disease. Adv Exp Med Biol. 2019;1175:335-53.
38. Akhter R, Shao Y, Formica S, Khrestian M, Bekris LM. TREM2 alters the phagocytic, apoptotic and inflammatory response to Abeta(42) in HMC3 cells. Mol Immunol. 2021;131:171-9.
39. Hjorth E, Frenkel D, Weiner H, Schultzberg M. Effects of immunomodulatory substances on phagocytosis of abeta(1-42) by human microglia. Int J Alzheimers Dis. 2010;2010.
40. Park JY, Paik SR, Jou I, Park SM. Microglial phagocytosis is enhanced by monomeric alpha-synuclein, not aggregated alpha-synuclein: implications for Parkinson's disease. Glia. 2008;56(11):1215-23.
41. scientific T. pHrodo Indicators for pH Determination.
42. Leinenga G, Koh WK, Gotz J. A comparative study of the effects of Aducanumab and scanning ultrasound on amyloid plaques and behavior in the APP23 mouse model of Alzheimer disease. Alzheimers Res Ther. 2021;13(1):76.
43. Vaz M, Silva V, Monteiro C, Silvestre S. Role of Aducanumab in the Treatment of Alzheimer's Disease: Challenges and Opportunities. Clin Interv Aging. 2022;17:797-810.
44. Sevigny J, Chiao P, Bussiere T, Weinreb PH, Williams L, Maier M, et al. The antibody aducanumab reduces Abeta plaques in Alzheimer's disease. Nature. 2016;537(7618):50-6.
45. Andreone BJ, Larhammar M, Lewcock JW. Cell Death and Neurodegeneration. Cold Spring Harb Perspect Biol. 2020;12(2).
46. Qiu Z, Zhang H, Xia M, Gu J, Guo K, Wang H, et al. Programmed Death of Microglia in Alzheimer's Disease: Autophagy, Ferroptosis, and Pyroptosis. J Prev Alzheimers Dis. 2023;10(1):95-103.
47. Cell Culture FAQs. In vitro technologies.
48. Dravid A, Raos B, Svirskis D, O'Carroll SJ. Optimised techniques for high-throughput screening of differentiated SH-SY5Y cells and application for neurite outgrowth assays. Sci Rep. 2021;11(1):23935.
49. Dello Russo C, Cappoli N, Coletta I, Mezzogori D, Paciello F, Pozzoli G, et al. The human microglial HMC3 cell line: where do we stand? A systematic literature review. J Neuroinflammation. 2018;15(1):259.
50. Iovino L, Tremblay ME, Civiero L. Glutamate-induced excitotoxicity in Parkinson's disease: The role of glial cells. J Pharmacol Sci. 2020;144(3):151-64.
51. Nampoothiri M, Reddy ND, John J, Kumar N, Kutty Nampurath G, Rao Chamallamudi M. Insulin blocks glutamate-induced neurotoxicity in differentiated SH-SY5Y neuronal cells. Behav Neurol. 2014;2014:674164.
52. Belov Kirdajova D, Kriska J, Tureckova J, Anderova M. Ischemia-Triggered Glutamate Excitotoxicity From the Perspective of Glial Cells. Front Cell Neurosci. 2020;14:51.
53. Bharate SS, Kumar V, Singh G, Singh A, Gupta M, Singh D, et al. Preclinical Development of Crocus sativus-Based Botanical Lead IIIM-141 for Alzheimer's Disease: Chemical Standardization, Efficacy, Formulation Development, Pharmacokinetics, and Safety Pharmacology. ACS Omega. 2018;3(8):9572-85.
54. Yuksel TN, Yayla M, Halici Z, Cadirci E, Polat B, Kose D. Protective effect of 5-HT7 receptor activation against glutamate-induced neurotoxicity in human neuroblastoma SH-SY5Y cells via antioxidative and antiapoptotic pathways. Neurotoxicol Teratol. 2019;72:22-8.
55. Sun X, Shi X, Lu L, Jiang Y, Liu B. Stimulus-dependent neuronal cell responses in SH-SY5Y neuroblastoma cells. Mol Med Rep. 2016;13(3):2215-20.

56. Pan XD, Zhu YG, Lin N, Zhang J, Ye QY, Huang HP, et al. Microglial phagocytosis induced by fibrillar beta-amyloid is attenuated by oligomeric beta-amyloid: implications for Alzheimer's disease. Mol Neurodegener. 2011;6:45.
57. Dahlgren KN, Manelli AM, Stine WB, Jr., Baker LK, Krafft GA, LaDu MJ. Oligomeric and fibrillar species of amyloid-beta peptides differentially affect neuronal viability. J Biol Chem. 2002;277(35):32046-53.
58. Heinitz K, Beck M, Schliebs R, Perez-Polo JR. Toxicity mediated by soluble oligomers of beta-amyloid(1-42) on cholinergic SN56.B5.G4 cells. J Neurochem. 2006;98(6):1930-45.
59. Tolar M, Abushakra S, Hey JA, Porsteinsson A, Sabbagh M. Aducanumab, gantenerumab, BAN2401, and ALZ-801-the first wave of amyloid-targeting drugs for Alzheimer's disease with potential for near term approval. Alzheimers Res Ther. 2020;12(1):95.
60. Gomez-Ramos A, Diaz-Hernandez M, Cuadros R, Hernandez F, Avila J. Extracellular tau is toxic to neuronal cells. FEBS Lett. 2006;580(20):4842-50.
61. Pieri L, Madiona K, Bousset L, Melki R. Fibrillar alpha-synuclein and huntingtin exon 1 assemblies are toxic to the cells. Biophys J. 2012;102(12):2894-905.
62. Zhang H, Cao Y, Ma L, Wei Y, Li H. Possible Mechanisms of Tau Spread and Toxicity in Alzheimer's Disease. Front Cell Dev Biol. 2021;9:707268.
63. Wong YC, Krainc D. alpha-synuclein toxicity in neurodegeneration: mechanism and therapeutic strategies. Nat Med. 2017;23(2):1-13.
64. Reiss AB, Arain HA, Stecker MM, Siegart NM, Kasselman LJ. Amyloid toxicity in Alzheimer's disease. Rev Neurosci. 2018;29(6):613-27.
65. Pallo SP, DiMaio J, Cook A, Nilsson B, Johnson GVW. Mechanisms of tau and Abeta-induced excitotoxicity. Brain Res. 2016;1634:119-31.
66. Maezawa I, Zimin PI, Wulff H, Jin LW. Amyloid-beta protein oligomer at low nanomolar concentrations activates microglia and induces microglial neurotoxicity. J Biol Chem. 2011;286(5):3693-706.
67. Wang J, Wang F, Mai D, Qu S. Molecular Mechanisms of Glutamate Toxicity in Parkinson's Disease. Front Neurosci. 2020;14:585584.
68. Uff CEG, Patel K, Yeung C, Yip PK. Advances in Visualizing Microglial Cells in Human Central Nervous System Tissue. Biomolecules. 2022;12(5).
69. Honarpisheh P, Lee J, Banerjee A, Blasco-Conesa MP, Honarpisheh P, d'Aigle J, et al. Potential caveats of putative microglia-specific markers for assessment of age-related cerebrovascular neuroinflammation. J Neuroinflammation. 2020;17(1):366.
70. Vankriekelsvenne E, Chrzanowski U, Manzhula K, Greiner T, Wree A, Hawlitschka A, et al. Transmembrane protein 119 is neither a specific nor a reliable marker for microglia. Glia. 2022;70(6):1170-90.

APPENDIX

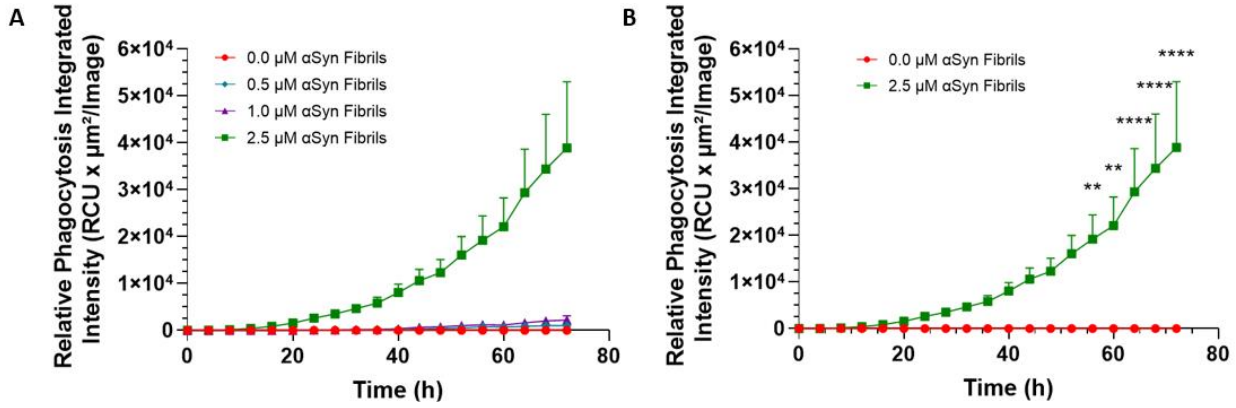

Figure S1: αSyn Fibrils increase phagocytosis in HMC3 PD model *in vitro* imaged with IncuCyte S3 Live-Cell Analysis System. A HMC3 cells phagocytosis fαSyn^{pH}. **B** HMC3 cells significantly phagocytose fαSyn^{pH} in a PD HMC3 model after 56 h compared to baseline (0.0 µM fibrils) (**p=0.005) and after 64 h (**** p< 0.0001). Data was obtained from IncuCyte S3 Live-Cell Analysis System. Phagocytic capacity was quantified as the relative phagocytosis integrated intensity, *i.e.*, fluorescence compared to initial time (t=0) fluorescence. Data points represent mean±SEM, with n=3 per condition. Two-Way ANOVA Dunnett's-multiple comparisons test.

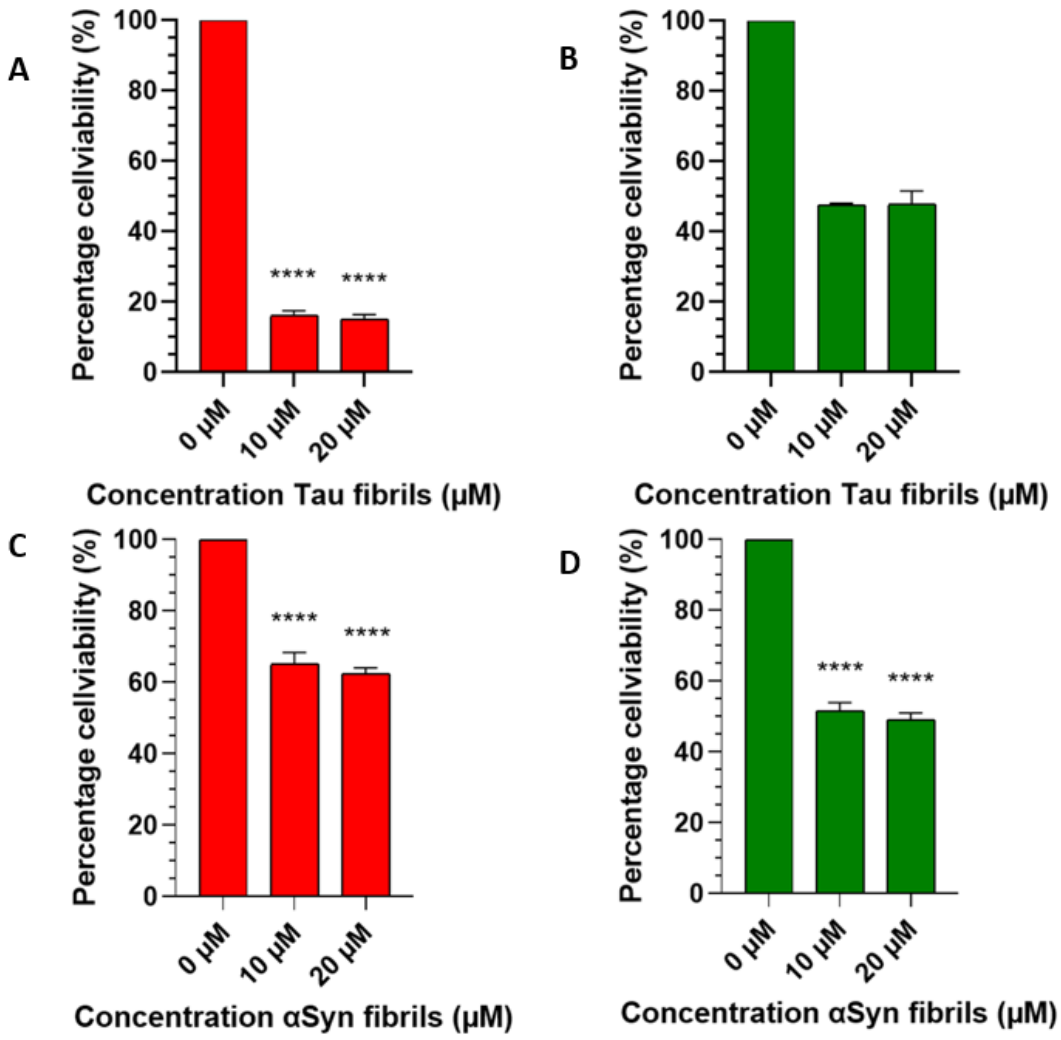

Figure S2: Cell viability was decreased by induction of αSyn and Tau fibrils measured with MTT. A Tau fibrils significantly decreases cell viability in SH-SY5Y cells. Each column represents mean±SEM of n=3 per condition. One-Way ANOVA with Dunnett's multiple comparisons test. **B** Tau fibrils positively decrease cell viability in HMC3 cells. Each column represents mean±SEM of n=2 per condition. Kruskal-Wallis-test. **C** αSyn fibrils significantly decrease cell viability in SH-SY5Y cells. Each column represents mean±SEM of n=4 per condition. One-Way ANOVA with Dunnett's multiple comparisons test. **D** αSyn fibrils significantly decreased cell viability in HMC3 cells. Each column represents mean±SEM of n=3 per condition. One-Way ANOVA with Dunnett's multiple comparisons test. Asterisks indicate statistically significant differences (****p <0.0001, ***p<0.001, **p=0.005 and *p=0.05). Data was obtained with MTT assay measured on a GloMax microplate reader.

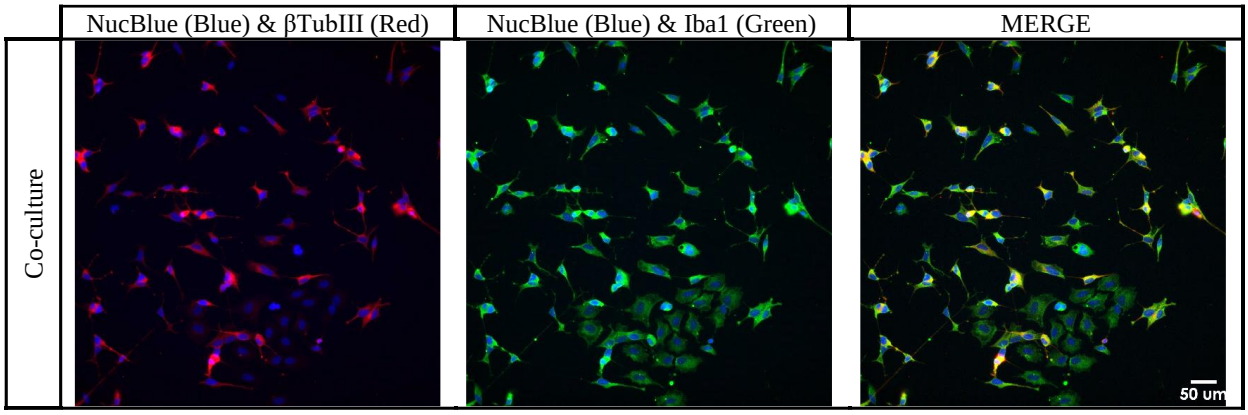

Figure S3: Markers on co-culture. SH-SY5Y cells are selectively stained with βTubIII (Red). However, HMC3 cells are not selectively stained with Iba1 (Green). NucBlue (Blue) staining was used to stain all cell nuclei. Images were obtained at 20X magnification using the ImageXpress Micro 4. Scale bar, 50 µm.